

# Degradation of inkjet ink by greensand and ultrasonic sonification

Mirela Rožić<sup>1</sup>, Marina Vukoje<sup>1</sup>, Kristinka Vinković<sup>2</sup>, Nives Galić<sup>2</sup>, Mirela Jukić<sup>3</sup>

<sup>1</sup> University of Zagreb Faculty of Graphic Arts, Getaldićeva 2, Zagreb, Croatia

<sup>2</sup> University of Zagreb Faculty of Science, Department of Chemistry, Horvatovac 102a, Zagreb, Croatia

<sup>3</sup> Andrija Stampar Teaching Institute of Public Health, Mirogojska 16, Zagreb, Croatia

## Abstract

The study describes the degradation of inkjet ink at low frequency ultrasound (US) and greensand to compare their reactivity. Environmental sonochemistry is a rapidly growing area and an example of the advanced oxidation process (AOP) that deals with the destruction of organic species in aqueous solutions. Greensand is a granular material coated with a thin layer of manganese dioxide ( $\text{MnO}_2$ ) which is among the strongest natural oxidants. In our study magenta inkjet water-based printing ink was dissolved in distilled water and the solutions obtained after degradation were analysed in terms of total organic compound (TOC) and absorption curves in the visible spectra. Also used for the process monitoring was high performance liquid chromatography (HPLC). The efficiency of discoloration is significantly affected by the effluent pH. The efficiency of discoloration was higher when the pH of initial solution was 2 with respect to the initial solution pH of 5.5. In all solutions, irrespective of the initial pH value and the processing method the oxidation of polyhydric alcohols occurs. Although the decomposition is significant, surface peaks resulting from HPLC analysis are very small. Decolourization is closely related to the cleavage of the  $-\text{C}=\text{C}$  and  $-\text{N}=\text{N}-$  bonds, and oxidation of polyhydric alcohol to the formation of monosaccharides, carboxylic acids or other low molecular weight compounds with a lesser number of unsaturated double bonds. These compounds have low UV absorbance or they absorb below 200 nm and therefore their detection is impossible. Thus, the obtained total organic compound results indicate a small degree of mineralization. The effectiveness of the low-frequency ultrasound (20 kHz) oxidation is similar to the effectiveness of oxidation by greensand.

**Key words:** oxidation, ultrasound, greensand, inkjet printing ink

## 1. Introduction

Wastewater effluents in some industries, such as dyestuff, textiles, leather, paper, and plastics contain several kinds of synthetic dyestuffs. The presence of colour in water for whatever use is undesirable (Guzman-Duque et al., 2011). Even with the presence of very small amounts of dyes in water (less than  $1\text{ mg dm}^{-3}$  for some dyes) the colour is highly visible (Wu et al., 2013) and can be toxic for life and harmful for human beings. Hence, the removal of colour from process or waste effluents is an issue of fundamental importance for the environment (Mohamed et al., 2007, Wu et al., 2013, Vončina Brodnjak and Majcen-Le-Marechal, 2003). Until now, conventional methods such as coagulation, microbial degradation, absorption on activated carbon, incineration, biosorption,

filtration, and sedimentation have been used to treat dye wastewater. During the last two decades, Advanced Oxidation Processes (AOPs) have emerged as sludge-free alternatives for decolourizing azo dyes (Eren and Ince, 2010). Ultrasound is considered to be an advanced oxidation process (AOP) that generates  $\text{OH}\cdot$  radicals through acoustic cavitation (Eren, 2012). The sonochemical effect takes place at the gase/liquid interface due to the oxidation of organic molecules by  $\text{OH}\cdot$  and, to a lesser extent, in the bulk solution or the pyrolytic decomposition inside the bubbles. Hydrophilic and non-volatile compounds such as dyes mainly degrade through OH-mediated reactions in the bulk solution and at the bubble-liquid interface, while hydrophobic and volatile species degrade

thermally inside the bubbles (Eren, 2012; Moumeni et al., 2012).

Researchers have shown that high frequencies are usually effective in degrading hydrophilic and non-volatile organics such as dyes, while low frequencies are more suitable for hydrophobic and volatile compounds. The result was attributed to a larger number of oscillations at high frequency that allowed a larger fraction of OH-ejection into the bulk liquid (Rehorek, 2004; Eren, 2012; Eren and Ince, 2010).

According to Guzman-Duque et al. (2011) by-products of aromatic structures occurred as a result of sonochemical degradation of crystal violet dye in water. As demonstrated by Siddique et al. (2011) sonoelectrochemical treatment of un-hydrolyzed reactive blue 19 dye for 30 min resulted in the formation of acetic acid, benzoic acid, etc. For hydrolyzed dye, a treatment of 10 min was enough. According to Moumeni et al. (2012) sonochemical degradation of malachite green occurs via two competitive processes: N-demethylation and destruction of the conjugated structure.

Greensand is a granular material, coloured in purple-black, derived from glauconite. Glauconite is a very common mineral in the class of zeolite, coated with a thin layer of manganese dioxide ( $\text{MnO}_2$ ). Manganese oxides are among the strongest natural oxidants in soils and sediments with a reducing potential between 1.27 and 1.50 V. They are capable of oxidizing many inorganic pollutants and a wide range of organic compounds such as phenols, aromatic amines, antibiotics, alcohol and colorants (Wang et al., 2014; Markovski et al., 2014; Zhang et al., 2013; Hao et al., 2013; Clarke et al., 2013; Qu et al., 2014; Zhua et al., 2010; Wang et al., 2017; Jiang et al., 2016; Das and Bhattacharyya, 2014; Fang et al., 2016; Dang et al., 2016).

Every inkjet formulation contains ingredients to preserve the colorant in a wet, fluid medium, whether solvent or carrier. Thus, water as a neutral fluid adjusts viscosity, adds volume, and allows the regulation of the concentration of the dye formulation. Then we have the surfactant and acid or alkali (base) to control the pH of the formulation (Cie, 2015). Water-based inkjet printing inks are comprised of colourant (dye or pigment), additives, humectants (ethylene glycol, polyethylene glycol, triethylene

glycol or diethanolamine) and water. Originally coloured liquids (dye-based colourants) are fully dispersed and dissolved in water (Aldib, 2015).

About 50% of the dyes produced in the world are derived from azo compounds. The main characteristic of this family of compounds is the presence of the azo group ( $-\text{N}=\text{N}-$ ), which allows larger extension of  $\pi$ -electronic conjugation and, therefore, intense absorption of light in the visible region of the electromagnetic spectrum (Ferreira, 2013). In water-based ink jet printing inks the anionic dyes are mostly used as colourants (Ferreira, 2013). Azo dyes themselves are not toxic. Under anaerobic conditions azo dyes are cleaved by microorganisms to form potentially carcinogenic aromatic amines. Aromatic amine formation may be avoided by the use of oxidative processes (Rehorek et al., 2004).

The oxidation of a mono-component system is the subject-matter of research of most of the authors of this paper. Thus, the oxidation of the real system, which consists of different organic components is presented. We studied the degradation of the components from a solution obtained by dissolving an inkjet water-based printing ink (dye-based) in distilled water. The oxidation process was conducted with greensand batch process and ultrasonic irradiation (low frequency ultrasound). The comparison of the effectiveness of the presented oxidation processes was given.

## 2. Material and methods

### 2.1 Model solution

Dye solution with a concentration of  $100 \text{ mg dm}^{-3}$  was prepared by dissolving of the magenta inkjet printing ink (Epson Stylus Pro 7000) in distilled water. According to the producer, the approximate composition of printing ink is as follows: 1.5% dye; 8% glycerol ( $\text{OHCH}_2\text{CH}(\text{OH})\text{CH}_2\text{OH}$ ), 28% ethilenglycol [ $(\text{CH}_2)_2(\text{OH})_2$ ], 1% urea and 61.5% water.

### 2.2 Chemicals

The chemicals used have the purity of the corresponding analytical grade from producer "Kemika" Zagreb. Distilled water with the electrical conductivity of less than  $1 \text{ mS cm}^{-1}$  was also used. For adjusting the dyestuffs' pH value

to 2.0 H<sub>2</sub>SO<sub>4</sub> solution the concentration of 2 mol dm<sup>-3</sup> was used.

## 2.3 Apparatus

Total organic carbon analyzer, (TOC-V<sub>CHN/CSN</sub>, Shimadzu Corporation, Japan) was used for TOC concentration measurements. pH value was measured using inoLab\_IDS, Multi 9310. Dyestuff model solutions were mixed using the rotary shaker Edmund Bühler GmbH. Ultrasonic sonification was conducted using Sonopuls HD 3100 ultrasound with frequency of 20 kHz. The spectral absorption curves were determined with Konica Minolta Spectrophotometer CM-3600d. UV-Vis spectrometry was performed with a Perkin Elmer, Lambda 10 spectrophotometer. The spectra were recorded between 200 and 800 nm at a scan rate of 240 nm min<sup>-1</sup>.

The HPLC analyses were carried out on Agilent 1100 Series system consisting of quaternary pump, vacuum degasser, autosampler, thermostated column oven and multichannel UV diode-array detector (Agilent Technologies, Palo Alto, CA, USA). Chromatographic separation was carried out on a Zorbax Eclipse XDB column (150 mm × 4.6 mm) with C<sub>18</sub> functional groups and 5 μm particle size (Agilent Technologies, Palo Alto, CA, USA). The column temperature was 40 °C, injection volume 50 μL, flow rate of the mobile phase 1 mL min<sup>-1</sup>, and the time of analysis 43 min. The mobile phases A (0.34 g TBASH + 900 mL water + 100 mL acetonitrile) and B (acetonitrile) were used for gradient elution as follows: the initial ratio of 25 % of acetonitrile was held constant for 5 min, then the ratio of acetonitrile was increased to 40 % over the following 8 min, and to 90 % in the following 17 min, held constant for 10 min and decreased to the initial value of 25 % over 0.5 min. The analytes were detected by monitoring the UV absorbance at 204 nm, 238 nm, 287 nm and 538 nm, which were set according to the UV absorption spectra of the initial sample solution.

## 2.4. Analytical procedure

### 2.4.1 Greensand oxidation treatment

Experiments were conducted in batch reactors at 25°C. 0.25 g of greensand was placed into the plastic laboratory containers (50 cm<sup>3</sup>) and

covered with 25 cm<sup>3</sup> dyestuff solution. The solution was shaken on rotary shaker at a speed of 250 rotation/min during 10, 30, 60 and 220 min.

### 2.4.2. Ultrasonic oxidation treatment

25 cm<sup>3</sup> of dyestuff solution was placed into the laboratory beakers. The power of ultrasound was adjusted to 30, 80 and 150 W. Duration of treatment was 10, 20 and 30 min.

After treatments, all the solutions were centrifugated and in the obtained supernatants the TOC was determined and the absorption spectra were acquired in the visible spectral range. The HPLC analyses were used to monitor the initial and degradation products visible by the UV-VIS absorption detection. 50 μL of each sample was injected on the column, without any preparation or dilution.

## 3. Results and discussion

### 3.1 Oxidation by greensand

Figure 1 presents the TOC concentration measurements in original dyestuff solution and in all solutions treated with greensand. The initial pH values of dyestuff solutions were 5.5 and 2.0.

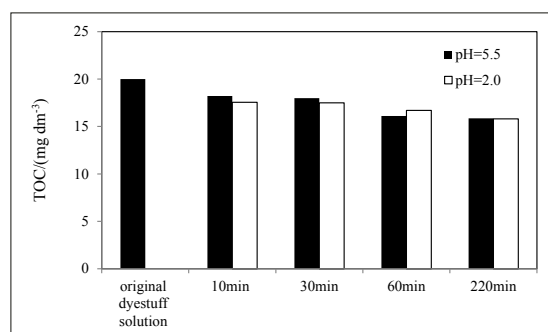


Fig.1.

After 10 minutes of treatment, the TOC concentrations were lower but this is negligible, as well as the further reduction which appeared with the increase of shaking time. The original dyestuff solution has TOC concentration of 20 mg dm<sup>-3</sup>. After 220 min of shaking, the TOC concentration in dyestuff solution with pH value 5.5 decreased to 15.87 mg dm<sup>-3</sup>. The efficiency of TOC removal was around 20%. The solution was slightly less coloured compared to original solution but complete discoloration didn't occur. The removal of TOC in dyestuff solution with initial pH value of 2.0 is

approximately the same as in the initial dye-stuff solution with a pH value of 5.5. However, in acidic solutions discoloration has occurred (Figure 2).

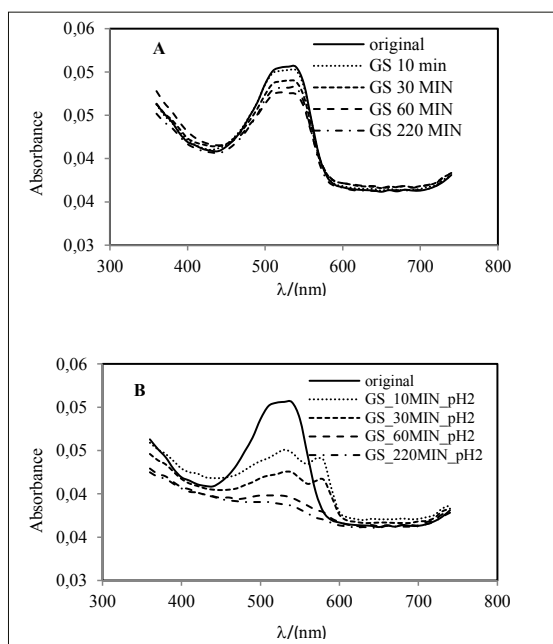


Fig.2.

Figure 2 shows the absorption spectra of dye-stuff solutions. A slight reduction of the absorption maximum of the initial solution with pH 5.5 (Figure 2A) and a significant reduction

of the absorption maximum in acidic solutions (Figure 2B) were observed.

Table 1 shows the recording wavelengths and retention times of 19 components monitored by the HPLC analysis.

The chromatograms of the initial solution recorded at 204 and 538 nm are shown in Figure 3. The peak with the retention time of 11.9 minutes represents the colour which is verified by recording its UV spectra during HPLC analysis using the diode array detector.

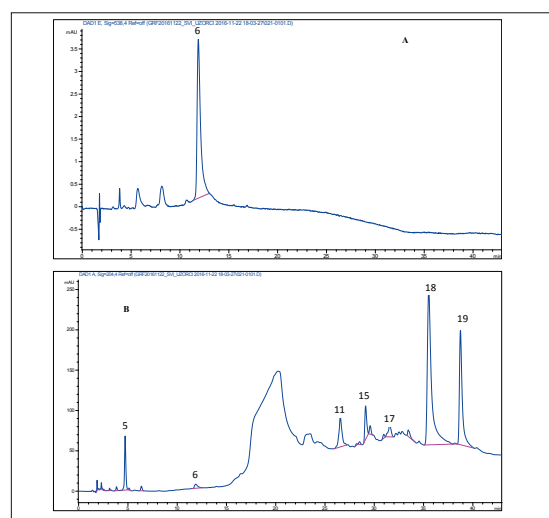


Fig.3.

Table 1

Peak No.	$t_R$ / (min)	$\lambda_{max}$ / (nm) wavelength of maximum absorption obtained from the recorded spectra	$\lambda_{max}$ / (nm) wavelength at which a certain peak was recorded, i.e. in which the determined peak area was used in the results
1	A	204, 310	204
2	D	204	204
3	D	220, 250, 330	204
4	I	230, 275, 530	204
5	I	204, 230, 300	204
6	I (dye)	220-230, 280, 510-545	204
7	D	204	204
8	D	204	204
9	D	204, 230, 280	287
10	I	240-250	238
11	I	204, 230, 275	204
12	I	230	238
13	I	240, 250, 320, 345	238
14	I	280	287
15	I	204	204
16	I	204, 240, 305,	204
17	I	204, 300	204
18	I	204, 225, 260	204
19	I	204, 230, 275	204

Chromatogram of the initial solution contained 13 peaks recorded at different wavelengths. The components with the retention times of 2.05 min, 3.1 min, 16.4 min, 23.5 min i 24.5 min (peaks # 2, 3, 7, 8 and 9) were not detected in the initial sample solutions, but only in the solutions after treatment, so these components might be considered as degradation products (Table 1). A peak with the retention time of 1.3 min which is not present in the initial sample solution appears only in the acidified solutions, and probably relates to the sulphuric acid (Table 1). Other peaks belong to other components in the solution (alcohols). Two components with retention times of 35.5 and 38.7 minutes (peaks # 18 and 19) have significantly higher peak areas than the other peaks. These are probably the prevalent components in the samples (or the components with significantly higher UV absorbance than all other components). The components with the retention times of 4.7 min, 26.5 min, 29.1 min, 29.5 and 31.5 min (peaks # 5, 11 and 15-17) have lower peak areas than the previous two, but still significant and probably related to less concentrated compounds in the samples. The areas of the compounds with the retention times of 3.8 min, 25.4 min, 27.1 min, 27.7 min and 28.5 min are much lower than all the other peaks. These probably appertain to compounds with very low concentration or UV-VIS absorption (peaks # 4, 10, 12, 13, 14).

The surface areas of all the peaks that appear in the original dyestuff solution are reduced upon treatment with greensand (Table 2) regardless to the initial pH value of solution except for peak # 6 (dye).

Table 2

Peak No.	Retention time/(min)	Peaks surface areas				
		Original dyestuff	30 min pH 5.5	10 min pH 2	20 min pH 2	
1	A	1.3	0	0	238.9	216
2	D	2.05	0	0	113.9	123
3	D	3.1	0	0	68.5	55.7
4	I	3.8	26.5	0	20.5	25.9
5	I	4.7	649	45.5	168.6	157.6
6	I (dye)	11.9	115.6	136.4	0	0
7	D	16.4	0	0	60.8	74
8	D	23.5	0	324.5	326.1	327.7
9	D	24.5	0	31.8	31.4	31.9
10	I	25.4	137.1	54.1	53.6	54.9
11	I	26.5	1162	286.3	308.5	365.8

12	I	27.1	60.5	27.2	27.4	27.9
13	I	27.7	60.9	25.4	25.6	26
14	I	28.5	292	108.6	108.8	110.5
15	I	29.1	862.2	215.1	216.3	218.4
16	I	29.5	931.7	52.7	53.6	54.5
17	I	31.5	891.2	128.7	134.1	132.2
18	I	35.5	5705.5	2472.6	2494.4	2507.2
19	I	38.7	3054.2	1146.6	1155.3	1159.5

Area of peak # 6 is not reduced in a solution of pH 5.5, which means that there is no degradation of dyes. These results confirm the resulting absorption curve. Moreover, surface area of this peak is slightly higher. The total area of all peaks obtained by HPLC analysis of the original dyestuff solution is 13948.4. After greensand oxidation treatment of the original dyestuff solution (pH = 5.5) for 30 minutes, the total peak area is reduced to 4699.2. This means that the concentration of components in the solution has decreased by 66.3%. The surface area of resulting peaks was 356.3 representing only 2.5% of the initial surface. The greatest reduction of the peak surface areas was obtained for the peaks #5, 11, 15-17 in the neutral solution as well as for acid solution (from 75 to approximately 95% compared to the initial surface area of individual peaks, Table 3).

Table 3

Peak No.	Retention time/(min)	% of degradation			
		30 min pH 5.5	10 min pH 2	20 min pH 2	
4	I	3.8	100.0	22.6	2.3
5	I	4.7	93.0	74.0	75.7
6	I (dye)	11.9	-18.0	100.0	100.0
10	I	25.4	60.5	60.9	60.0
11	I	26.5	75.4	73.5	68.5
12	I	27.1	55.0	54.7	53.9
13	I	27.7	58.3	58.0	57.3
14	I	28.5	62.8	62.7	62.2
15	I	29.1	75.1	74.9	74.7
16	I	29.5	94.3	94.2	94.2
17	I	31.5	85.6	85.0	85.2
18	I	35.5	56.7	56.3	56.1
19	I	38.7	62.5	62.2	62.0

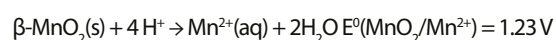
Other components are degraded in smaller percentage (from about 55 to 63%). Following the treatment of the acidic dyestuff solution with greensand for 10 minutes, the total surface area of the peaks obtained by HPLC analysis of the original dyestuff solution has decreased to 4766.7. The surface area reduction is 65.8%. The resulting surface is around 600.7.

After treatment of the acidic dyestuff solution with greensand for 20 minutes, the total surface area of the peaks present in the original dyestuff solution has decreased to 4840.4. The surface area reduction is 65.3%. The resulting surface is around 538.3. Slightly larger resulting surface areas of the peaks in the acidic dyestuff solution can be attributed to the decomposition of dyes and production of its degradation products (peaks #2, 3 and 7; Table 2). Although the decomposition is significant and most likely outlines the alcohol degradation, resulting surface peaks are very small.

However, it is possible that during degradation of these components the formed products of decompositions at the tested wavelengths have little or no absorbance and therefore their detection is impossible. HPLC analysis results of the dyestuff solution after shaking with the greensand (Table 2) did not differ significantly. Based on the obtained TOC results, we can assume that there was a slight mineralization.

Monosaccharides and carboxylic acid are formed by oxidation of polyhydric alcohols. Monosaccharides are the first oxidation products of polyhydric alcohols. All of these compounds are very easily oxidized. According to Elmaci et al. (2017) nano-manganese ferrite-supported manganese oxide catalyst can oxidize benzyl alcohol and benzaldehyde without employing any oxidizing agent other than the air present in the reactor. Similar results were obtained by Massa et al. (2012). As demonstrated by Wieland et al. (1996) CO<sub>2</sub>, glycolic acid, and adsorbed CO are identified as reaction products for ethylene glycol and glycolaldehyde oxidation by platinum. According to Giroto et al. (2010) the photodegradation of poly-ethylene glycol (PEG) and aqueous solutions by means of photo-Fenton and H<sub>2</sub>O<sub>2</sub> / UV processes forms acetic, formic and glycolic acid.

One of the reasons for a better discoloration of a dyestuff solution in acidic media is possibly the increase of MnO<sub>2</sub> reduction potential. Reduction potential of Mn oxides is changed according to the Nernst equation:



In accordance with the Nernst equation, pH reduction increases the reduction potential of Mn oxides. Another reason for a better discoloration in an acidic media is the surface

exchange, protonation / deprotonation of Mn oxide with pH. In the common case when the surface charge-determining ions are H<sup>+</sup>/OH<sup>-</sup>, the net surface charge is affected by the pH of the liquid in which the solid is submerged. The pH (at 25°C) of the isoelectric point for manganese (IV) oxide in water is 4-5. At pH values less than 4-5, the surface of MnO<sub>2</sub> is positively charged and in these conditions the attractive forces between the anionic dye molecules and positively charged MnO<sub>2</sub> particles surface enhance the diffusion of dye molecules from the bulk solution to the adsorbent surface. A third reason may be protonation of negatively charged dye sites, causing hydrophobicity increase of the dye molecules and possibly an easier degradation of such molecules. A possible reason is the fact that pH has an influence on the azo-hydrazo equilibrium of azo dyes. Acidic pH favours the hydrazo form (NH), while basic pH favours the more stable azo form (OH). In magenta dyes this plays an important role (Fryberg, 2005).

To establish a pH-dependent flocculation stability of ink jet dye in this study a pH-adjusted control was prepared. The pH 2 of dyestuff solution did not show any evidence of flocculation but after several months discolorization of magenta occurred, which was more pronounced under the light.

### 3.2. Oxidation by ultrasonic irradiation

Figure 4 shows the TOC concentration of the dyestuff solution after ultrasonic irradiation. TOC concentrations are similar to those obtained by greensand treatment, and a slight decrease in concentrations was observed regardless to the initial pH value and used power of ultrasound.

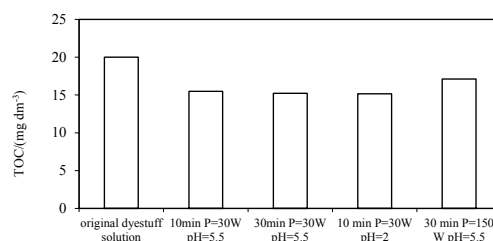


Fig.4.

From the absorption spectra of the dyestuff solution, a very low reduction of the absorption maximum in dyestuff solutions with initial pH

5.5 can be seen (Figure 5A) as well as a decrease of absorption maximum after the ultrasonic irradiation in acidic solution (Figure 5B).

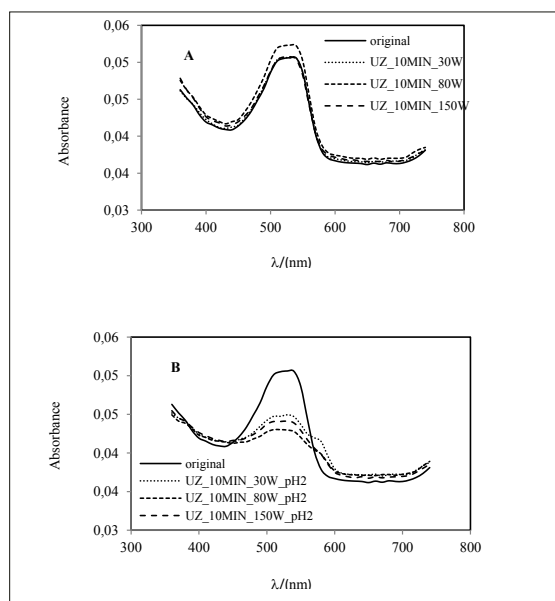


Fig.5.

Therefore, the results are very similar to those obtained after treatment with greensand. In acidic solution, a better decolourization is achieved. Table 4 shows the results of HPLC analysis. It is evident that after the treatment of dyestuff solutions with pH 5.5, the colour

of the solution is not reduced (the number of peaks 6), as confirmed by the spectral absorption curves.

Moreover, peaks surface areas were again slightly higher. After processing of dyestuff solution with pH 2, peaks # 6 disappear. Decolouration efficiency increased in acidic conditions, which was probably associated with the effect of protonation of negative charges in acidic medium and the hydrophobic character of the resulting molecule which enhanced its reactivity (Wu, 2013).

Table 5 shows the share of individual component degradation to the relative analyzed peak areas in the original dyestuff solution. The highest reduction of the peak surface areas was obtained for the peaks # 4-5, and 10-17 in the neutral and acidic dyestuff solutions (from 75 to about 95%). Therefore, the degradation effectiveness of these components is slightly better compared to treatment with greensand. The remaining components # 18 and 19 degrade in a percentage of approximately 55 to 63%, which is similar to that obtained after treatment with greensand. The total area of the peaks present in the original dyestuff solution decreased at high ultrasonic irradiation power of 30 W and at pH 5.5 and at pH 2 (10 minutes) as well as

Table 4

Peak No.		Retention time /min	Peak surface areas						
			Original dyestuff solution	pH 5.5 P=30W	pH 2 P=30W	10 min pH 5.5 P=80W	10 min pH 2 P=80W	10 min pH 2 P=150W	30 min pH 5.5 P=150W
1	A	1.3	0	0	197.5	0	244.5	145.8	0
2	D	2.05	0	93.5	104.1	0	103.4	62.2	0
3	D	3.1	0	41.5	64.1	118.1	13.5	53.4	23.9
4	I	3.8	26.5	0	0	88	0	11.3	13.1
5	I	4.7	649	0	0	47.6	0	10.8	0
6	I (D)	11.9	115.6	119.9	0	124	0	0	120.3
7	D	16.4	0	35.6	0	26.6	36.1	44.7	38.7
8	D	23.5	0	300.2	350.6	306.6	316	322	320.9
9	D	24.5	0	0	51.4	28.3	28.9	29.2	29.9
10	I	25.4	137.1	49.8	49.4	49.9	54.2	52	65.0
11	I	26.5	1162	436.1	374.1	377	356.9	364.6	389.4
12	I	27.1	60.5	0	0	25	26.1	26.6	26.7
13	I	27.7	60.9	0	0	24.3	25	25.2	24.7
14	I	28.5	292	97.5	94.6	102	104	107.6	105.2
15	I	29.1	862.2	193.4	257.4	201.8	206.7	211.3	209.0
16	I	29.5	931.7	0	0	48.8	50.5	51.8	51
17	I	31.5	891.2	130.8	51.6	133	136.2	131.1	126.9
18	I	35.5	5705.5	2286.5	2299.8	2349.6	2350.6	2568.7	2500.2
19	I	38.7	3054.2	1136	1140.7	1152.5	1141.7	1136.5	1142.8

Table 5

Peak No.		Retention time /min	% of degradation					
			10 min pH 5.5 P=30W	10 min pH 2 P=30W	10 min pH 5.5 P=80W	10 min pH 2 P=80W	10 min pH 2 P=150W	30 min pH 5.5 P=150W
4	I	3.8	100.0	100.0	-232.1	100.0	57.4	50.6
5	I	4.7	100.0	100.0	92.7	100.0	98.3	100.0
6	I(dye) (D)	11.9	-3.7	100.0	-7.3	100.0	100.0	-4.1
10	I	25.4	63.7	64.0	63.6	60.5	62.1	52.6
11	I	26.5	62.5	67.8	67.6	69.3	68.6	66.5
12	I	27.1	100.0	100.0	58.7	56.9	56.0	55.9
13	I	27.7	100.0	100.0	60.1	58.9	58.6	59.4
14	I	28.5	66.6	67.6	65.1	64.4	63.2	64.0
15	I	29.1	77.6	70.1	76.6	76.0	75.5	75.8
16	I	29.5	100.0	100.0	94.8	94.6	94.4	94.5
17	I	31.5	85.3	94.2	85.1	84.7	85.3	85.8
18	I	35.5	59.9	59.7	58.8	58.8	55.0	56.2
19	I	38.7	62.8	62.7	62.3	62.6	62.8	62.6

at pH 2 dyestuff solution under irradiation power of 80 W (10 minutes). The surfaces were reduced to 4450, 4267.6 and 4452 (by 68, 69.4 and 68%, respectively). In other cases, the reduction of the peak surface areas is about 66%. The resulting surfaces formed during degradation in acidic solutions were 3.6% (10 min, P = 80 W) to 4% (10 min, P = 30 W), while in pH 5.5 the dyestuff solutions were in a range from 2.7% (30 min, P = 150 W) to 3.4% (10 min, P = 80 W). Somewhat larger resulting peak surface areas in acidic solution can be again attributed to the degradation of dyes and the formation of its degradation products.

#### 4. Conclusions

Greensand has been proved as an oxidant with similar effectiveness compared to ultrasonic irradiation. In all the tested dyestuff solutions, regardless to the initial pH value, the oxidation of the polyhydric alcohols occurs. During the oxidation of polyhydric alcohols monosaccharides, carboxylic acids and other smaller molecules with few double bonds are probably formed. These compounds have lower UV absorbance or they absorb at wavelengths below 200 nm, which is very difficult to record because usually the mobile phase absorbs in this area, too. In neutral solutions a poor decolourization is present, which can be improved by acidification. Organic molecules which are coloured and absorb in the VIS electromagnetic spectral range have an expanded system of delocalized

$\pi$  electrons. Aromatic rings do not react easily without a catalyst and UV radiation. Thus, the cleavage of azo molecules probably occurs between two nitrogen atoms resulting in products with a different retention time and absorbance. Hence, the pH value is very important in inkjet water-based printing inks because it can significantly affect the stability of dyes.

#### 5. References

- Aldib, M., 2015. Photochromic ink formulation for digital inkjet printing and colour measurement of printed polyester fabrics. *Coloration technology*, 131, p. 172.
- Cie, C., 2015. *Ink Jet Textile Printing*. Woodhead Publishing Series in Textiles: Number 161. Woodhead Publishing.
- Clarkea, C. E., Kielarb, F., Johnsonc, K. L., 2013. The oxidation of acid azo dye AY 36 by a manganese oxide containing mine waste. *Journal of Hazardous Materials*, 246–247, p. 310.
- Dang, T.-D., Banerjee, A.N., Tran, Q.-T., R., Sudipta, (2016). Fast degradation of dyes in water using manganese-oxide-coated diatomite for environmental remediation. *Journal of Physics and Chemistry of Solids*, 98, p. 50.
- Das, M., Bhattacharyya, K.G., 2014. Oxidation of Rhodamine B in aqueous medium in ambient conditions with raw and acid-activated MnO<sub>2</sub>, NiO, ZnO as catalysts\* *Journal of Molecular Catalysis A: Chemical*, 391, p. 121.
- Eren, Z., 2012. Ultrasound as a basic and auxiliary process for dye remediation: a review. *Journal of Environmental Management*, 104, p. 127.



*Degradation of inkjet ink by greensand and ultrasonic sonification*

- Eren, Z., Ince N.H., 2010. Sonolytic and sonocatalytic degradation of azo dyes by low and high frequency ultrasound. *Journal of Hazardous Materials*, 177, p. 1019.
- Elmaci, G., Ozer, D., Zumreoglu-Karan, B., 2017. Liquid phase aerobic oxidation of benzyl alcohol by using manganese ferrite supported-manganese oxide nano-composite catalyst. *Catalysis Communications*, 89, p. 56.
- Fang, L., Hong R., Gao, J., Gu, C., 2016. Degradation of bisphenol A by nano-sized manganese dioxide synthesized using montmorillonite as templates. *Applied Clay Science*, 132–133, p. 155.
- Ferreira, G.R., Costa Garcia, H., Couri, M. R. C., Dos Santos, H.F., C. de Oliveira, L. F., 2013. On the Azo/Hydrazo Equilibrium in Sudan I Azo Dye Derivatives. *The Journal of Physical Chemistry A*, 117, p. 642.
- Fryberg, M., 2005. Dyes for ink-jet printing. *Rev. Prog. Color.*, 35, p. 1.
- Giroto, J.A., Teixeira, A.C.S.C., Nascimento, C.A.O., Guardani, R., 2010. Degradation of Poly(ethylene glycol) in Aqueous Solution by Photo-Fenton and H<sub>2</sub>O<sub>2</sub>/UV Processes. *Ind. Eng. Chem. Res.*, 49 (7), p. 3200.
- Guzman-Duque, F., Pétrier, C., Pulgarin, C., Peñuela, G., Torres-Palma, R.A., 2011. Effects of sonochemical parameters and inorganic ions during the sonochemical degradation of crystal violet in water. *Ultrasonics Sonochemistry* 18, p. 440.
- Hao, X., Zhao J., Zhao Y., Ma D., Lu, Y., Guo, J., Zeng, Q., 2013. Mild aqueous synthesis of urchin-like MnOx hollow nanostructures and their properties for RhB degradation. *Chemical Engineering Journal*, 229, p. 134.
- Jiang, L., Liu, L., Xiao, S., Chen, J., 2016. Preparation of a novel manganese oxide-modified diatomite and its aniline removal mechanism from solution. *Chemical Engineering Journal*, 284 (15), p. 609.
- Markovski, J. S., Marković, D. D., Đokić V. R., Mitrić, M., Ristić, M., Onjia, A. E., Marinković, A.D., 2014. Arsenate adsorption on waste eggshell modified by goethite,  $\alpha$ -MnO<sub>2</sub> and goethite/ $\alpha$ -MnO<sub>2</sub>. *Chemical Engineering Journal*, 237, p. 430.
- Massah, A., R., Kalbasi, R. J., Azadi, M., 2012. Highly selective oxidation of alcohols using MnO<sub>2</sub>/TiO<sub>2</sub>-ZrO<sub>2</sub> as a novel heterogeneous catalyst. *Comptes Rendus Chimie*, 15 (5), p. 428.
- Mohamed, M. M., Othman, I., Mohamed, R.M., 2007. Synthesis and characterization of MnO<sub>x</sub>/TiO<sub>2</sub> nanoparticles for photocatalytic oxidation of indigo carmine dye. *Journal of Photochemistry and Photobiology A: Chemistry*, 191, p. 153.
- Moumeni O., Hamdaoui O., Pétrier C., 2012. Sonochemical degradation of malachite green in water. *Chemical Engineering and Processing: Process Intensification*, 62, p. 47.
- Onat, T.A., H. Gümüşdere, T., Güvenç A., Dönmez G., Mehmetoğlu Ü., 2010. Decolorization of textile azo dyes by ultrasonication and microbial removal. *Desalination*, 255, (31), p. 154.
- Rehorek, A., Tauber, M., Gubitza G., 2004. Application of power ultrasound for azo dye degradation. *Ultrasonics Sonochemistry*, 11, p. 177.
- Siddique M., Farooq R., Khan, Z. M., Khan, Z., Shaukat, S.F., 2011. Enhanced decomposition of reactive blue 19 dye in ultrasound assisted electrochemical reactor. *Ultrasonics Sonochemistry*, 18 (1), p. 190.
- Qu, J., Shi, L., He, C., Gao, F., Li, B., Zhou, Q., Hu, H., Shao, G., Wang, X., 2014. Qiu, J., 2014. Highly efficient synthesis of graphene/MnO<sub>2</sub> hybrids and their application for ultrafast oxidative decomposition of methylene blue. *Carbon*, 66, p. 485.
- Vončina Brodnjak, D., Majcen-Le-Marechal, A., 2003. Reactive dye decolorization using combined ultrasound/H<sub>2</sub>O<sub>2</sub>. *Dyes and Pigments*, 59, p. 173.
- Wang, J., Li, J., Jiang, C., Zhou, P., Zhang, P., Yu, J., 2017. The effect of manganese vacancy in birnessite-type MnO<sub>2</sub> on room-temperature oxidation of formaldehyde in air. *Applied Catalysis B: Environmental*, 204 (5), p. 147.
- Wang, Y., Zhang, X., He X., Zhang, W., Zhang X., Lu, C., 2014. In situ synthesis of MnO<sub>2</sub> coated cellulose nanofibers hybrid for effective removal of methylene blue. *Carbohydrate Polymers*, 110 (22), p. 302.
- Wieland, B., Lancaster, J. P., Hoaglund, C. S., Holota, P., Tornquist, W. J., 1996. Electrochemical and Infrared Spectroscopic Quantitative Determination of the Platinum-Catalyzed Ethylene Glycol Oxidation Mechanism at CO Adsorption Potentials. *Langmuir*, 12 (10), p. 2594.
- Wu, T.Y., Guo N., Teh, C.Y., Hay, J.X.W., 2013. *Advances in Ultrasound Technology for Environmental Remediation*. Dordrecht Heidelberg New York London Springer.
- Zhang, T., Delai Sun, D., 2013. Removal of arsenic from water using multifunctional micro-/nano-structured MnO<sub>2</sub> spheres and microfiltration. *Chemical Engineering Journal*, 225, p. 271.
- Zhua, M-X., Wanga, Z., Xub, S.-H., Li, T., 2010. Decolorization of methylene blue by  $\beta$ -MnO<sub>2</sub>-coated montmorillonite complexes: Emphasizing redox reactivity of Mn-oxide coatings. *Journal of Hazardous Materials*, 181, p. 57.

---

This page was left blank intentionally!